J Mater Sci (2013) 48:6803–6810
DOI 10.1007/s10853-013-7485-4

Determination of nano-roughness of carbon fibers by atomic force microscopy

Jan Jäger · Judith Moosburger-Will · Siegfried Horn

Received: 13 February 2013 / Accepted: 29 May 2013 / Published online: 18 June 2013

Abstract We present a novel approach to determine the surface roughness on varying scales using atomic force microscopy data. The key factor is to find a suitable background correction for the desired scale. Using the example of the surface of sized and unsized high-tenacity carbon fibers, we present an easy method to find backgrounds for widely varying scales and to evaluate respective topography and surface roughness with the same lateral resolution as the microscope itself. The analysis is done by subtracting a tunable background from the respective height data. By choosing an appropriate background to investigate the surface topography of a carbon fiber on a nm-scale, only small nano-structures with a width of around 20 nm remain after the background subtraction. Evaluating the mean roughness R_a of these nano-structures, sized carbon fibers show an overall value of around 0.1 nm while unsized carbon fibers a value of around 0.4 nm. Total background corrected height analysis shows an even distribution of these nano-structures along the fibrils of the unsized fibers, whereas for the sized fibers the nano-structures are not present. The presented method allows analysis and visualization of the distribution of nano-structures on a carbon fiber surface for the first time. This feature is used to visualize the distribution of the sizing and can further be used to investigate the influence of different production parameters on the fiber topography or to evaluate the contribution of mechanical interlocking to the interfacial strength.

J. Jäger (✉) · J. Moosburger-Will · S. Horn
Experimental Physics II, Institute of Physics, University of Augsburg, 86135 Augsburg, Germany
e-mail: jan.jaeger@physik.uni-augsburg.de

Introduction

Surface roughness plays a major role in the adhesion between two materials. The scale of the roughness important for good adhesion varies depending on the materials used. For a good adhesion between mortar and concrete, a roughness with height differences of several mm is necessary [1]. In contrast, height differences in the micrometer range are important for the adhesion of glass to steel using a geopolymer [2]. For carbon fiber reinforced plastics (CFRPs), the interfacial strength between the fiber and the matrix is the key factor in their excellent mechanical properties such as high-specific modulus and tensile strength. The two major contributions to the interfacial strength are chemical bonding and mechanical interlocking. Chemical bonding, related to the presence, kind, and ratio of polar and dispersive groups is often considered to be more important than mechanical interlocking, which is related to the surface roughness of the carbon fiber [3–5]. On the other hand, surface roughness can play an important role because it improves mechanical interlocking and provides more adhesive surface [6–9]. Experiments on microcomposites have shown that friction, which is strongly related to surface roughness, plays a very important role in crack propagation and therefore for the tensile strength of the composite [10–12].

In general, the surface of high-tenacity carbon fibers is composed of characteristic structures on different scales. The fiber is roughly cylindrical with a diameter of around 7 μm. Depending on the manufacturing process, the surface of the fiber exhibits fibrils with a diameter of about 100 nm and orientated parallel to the fiber axes, structures on a scale of 10 nm, and on even smaller scales the edges of the basal planes. To protect the fiber surface and to improve the interfacial strength, carbon fibers are sized

after manufacturing. This step further changes the topography of the fiber surface. Until now, the correlation of surface structures with certain production parameters is not well understood. Contributing processes are polymerization of the precursor, spinning, stabilization, carbonization, and anodic surface oxidation.

Surface structures on all length scales contribute to the roughness of a carbon fiber. The surface roughness is usually determined using an atomic force microscope (AFM). In general, the calculated mean roughness R_a is obtained using a polynomial background subtraction in a several μm large image [3, 5]. Such polynomials are not able to consider small or local structures. The mean roughness is therefore determined by structures larger than 100 nm, i.e., fibrils, and is in the range of 5–50 nm. The role of much smaller structures with sizes of around 10 nm is not considered. Such nano-structures can be important because they increase the amount of adhesive surface and possibilities for mechanical interlocking. In addition to the roughness, which is a averaged over the whole image area, the spatial distribution of the nano-structures is of interest since it contains information about the production process of the fibers.

This study presents an easy to use tool for local analysis of surface structures of different orders of magnitude down to the nano-meter-scale by visualizing the smallest height differences. To this end a tunable, locally calculated background is subtracted from the height data, with the feature to subtract structures above a chosen scale. This allows the local evaluation of nano-structures and nano–roughness on an arbitrary large image for the first time. The lateral resolution of this method corresponds to the lateral resolution of the microscope itself. The presented method can be used to evaluate roughnesses and surface structures at widely different scales of any already existing height profiles.

In the case of carbon fiber, the influence of process parameters and changes in processes like anodic oxidation to plasma oxidation on the surface topography can be analyzed. Also, a deeper insight into the correlation between surface roughness and interfacial strength is expected. In this study, we apply the method to evaluate the spatial distribution of sizing on the fiber surface.

Experimental

Samples

The high-tenacity carbon fiber used in this study was provided by SGL Carbon, obtained in two different process states: after anodic oxidation (hereafter called UNS), and after sizing with an epoxy compatible polymer (hereafter called EPY). The sizing was washed away with methyl ethyl ketone in an ultrasonic bath for 1 h. The desized fibers are hereafter called EPYdeMEK.

Characterization

Atomic force microscopy images were taken with a Bruker Dimension Icon operating in standard tapping mode. The tips used had a nominal tip radius of 8 nm. The scan size of the images was 5 μm with a scan rate of 0.5 Hz and 1024 samples/line. The lateral resolution was about 10 nm, while the noise of the z-piezo was 35 pm. Analysis of the images was performed using Matlab® R2010a.

Varied scale background correction

Concept

The most important part in determining the surface roughnesses correctly is to find a good background correction. The background thereby has to fulfill some requirements. It first must be faithful to the original data. A second very important point is the local character of the background. Surface structures are in general not regularly distributed and also might only appear very locally. Thus, only a few neighboring data points should be relevant for the calculation of the background at one point, although, the parameters for the calculation have to be the same for the whole area. This requirement prevents the use of e.g., low-pass filters or fast Fourier transformation, because those techniques always consider the whole data set for their calculations and neglect the local character of surface structures. Because the background correction should work on arbitrary surfaces, the smoothness has to be an adjustable parameter.

In 2005, Eilers and Boelens[1] presented an easy and fast tool that had been originally developed to find the baselines for spectroscopic data, using a weighted (asymmetric) least square fitting with a Whittaker smoother [13, 14]. For the purpose of this study, the non-weighted (symmetric) approach is used:

$$S = \sum_i (y_i - z_i)^2 + \eta \sum_i (\Delta^2 z_i)^2 \quad (1)$$

$$\Delta^2 z_i = (z_i - z_{i-1}) - (z_{i-1} - z_{i-2}) \quad (2)$$

Here, y is the signal (sampled in equal intervals) and z the desired background, which can be obtained by minimizing S. Because we use the symmetric approach, the mean value of the background corrected signal will be close to 0. The smoothness of the background can be tuned with only one parameter, η, making its use very simple. Therefore, the

[1] Eilers PHC, Boelens HFM (2005) http://www.science.uva.nl/~hboelens/publications/draftpub/Eilers_2005.pdf

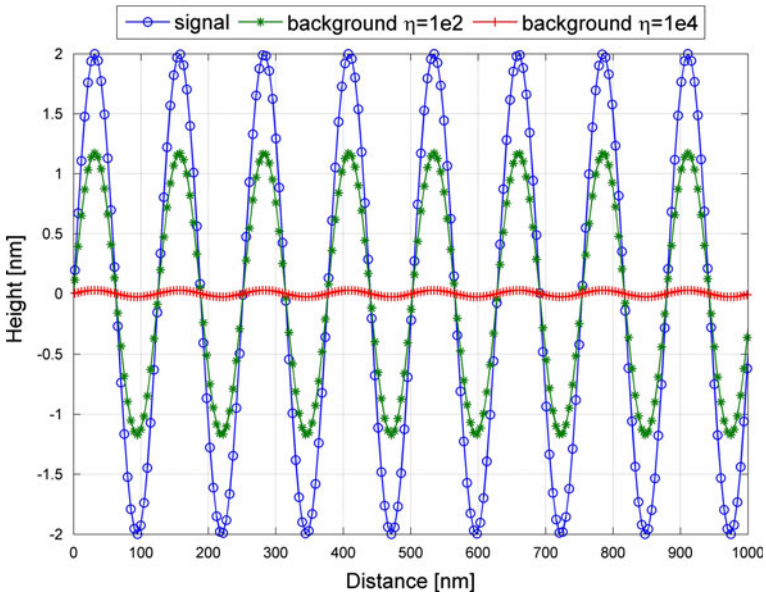

Fig. 1 Sinusoidal data signal and corresponding backgrounds for η = 1e2 and 1e4. The transmittances are 0.42 and 0.99, respectively

smaller η is, the smaller the mean distance between the data points and the background.

To demonstrate the power of the background calculation, we first apply it to a simulated surface. A sinusoidal curve is chosen for convenience. The surface roughness and the size of the surface structures can thereby be simulated by varying the wavelength and the amplitude.

Let y be a sinusoidal curve with 1024 points per 5 μm

$$y = B * sin(C * x) \tag{3}$$

The distance between two zero crossings (corresponding to the width of the surface structures) can be varied with parameter C, the amplitude (in nm) with the parameter B. Figure 1 shows an example for one sinusoidal data signal and two different backgrounds that differ in the value η in their calculations.

The wavelength of the curve in Fig. 1 is about 125 nm, thus, the simulated structures have a width of around 62 nm (= half wavelength). For η = 1e2, the background follows these structures quite well and only 42 % of the original signal would be remaining after background correction while for η = 1e4, 99 % would remain.

This so called transmittance, T, is defined as:

$$T = \frac{R_{a,\mathrm{corr}}}{R_{a,\mathrm{orig}}} \tag{4}$$

with $R_{a,\mathrm{corr}}$ and $R_{a,\mathrm{orig}}$ being the roughnesses R_a of the background corrected signal and the original signal, respectively. A transmittance of 0.9 represents an almost completely transmitted signal after background correction, while at a value of 0.1, the signal is almost completely subtracted. Table 1 gives an overview of the zero-crossing distances (in nm; see Eq. 3) for different values of η and calculated transmittances T.

Table 1 Overview of the zero-crossing distances from (3) (in nm) at certain values of η and calculated transmittances *T* after background correction

η	Transmittance *T*				
	0.9	0.7	0.5	0.3	0.1
1e5	170	260	320	390	570
1e4	100	145	180	225	320
1e3	55	83	103	128	178
1e2	33	48	58	70	103
1e1	19	25	32	40	56
1e0	9	14	18	22	32

By varying η, one can define the width of the structures which will be subtracted while smaller structures remain. As an example, an η value of 1e5 subtracts structures larger than 570 nm (10 % are transmitted), while the height of structures smaller than 170 nm remains unchanged within 10 %.

Application to carbon fiber surface

Carbon fibers are highly anisotropic and so are their surface structures. This fact prevents the use of a two-dimensional calculated background with one parameter η for both directions, because in this case all the structures would be subtracted. Instead, the presented one dimensional background is applied perpendicular to the fiber axes to preserve these structures.

Figure 2 shows a three-dimensional atomic force microscopy image of the surface of a typical high-tenacity carbon fiber. The surface profile (blue line) was background corrected with two different values of η (Fig. 3a,

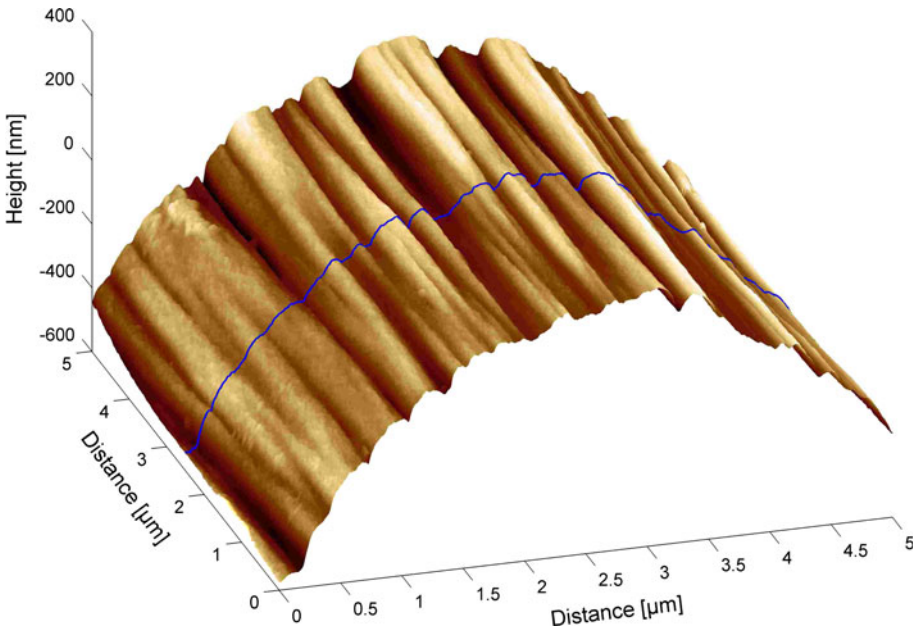

Fig. 2 Three-dimensional atomic force microscopy image of the surface of a typical high-tenacity carbon fiber showing its cylindrical shape and fibrillar substructures. The *blue line* marks the profile for Fig. 3a (Color figure online)

green and red lines), and the corrected surface profiles are shown in Fig. 3b.

The roughly cylindrical shape of a carbon fiber (diameter $\sim$7 µm, visible in Fig. 2) is completely subtracted at an η value of 1e5, but the fibrillar substructure (width $\sim$100 nm) remains almost unchanged. Whereas for an η value of 1e1, the fibrillar substructure is also subtracted and only much smaller nano-structures remain (compare Table 1). Comparing the main contributions to the mean roughness R_a of the original signal and the background corrected signals with η = 1e5 and 1e1, the R_a value of the original signal is dominated by the cylindrical shape. For an η value of 1e5, the fibrils are the dominating structures, while for an η value of 1e1, only nano-structures would show up in the mean roughness.

Thus, presented background is able to emphasize the anisotropic structures of widely varying scales by changing the parameter η.

Results and discussion

Multiscale roughness analysis

Ten surface images of each of the unsized (UNS) and sized (EPY) fibers were background corrected using different values of η between 1e0 and 1e6. The mean roughnesses R_a and corresponding standard deviations for the entire image, calculated after the respective background correction, are summarized in Table 2.

This multiscale analysis allows the calculation of the roughness values of structures with widely varying lateral sizes. η values of 1e6 and 1e5 result in emphasis of the fibrillar substructure. In these cases there are no differences in R_a between UNS and EPY. The thickness of the sizing must therefore be much less than 100 nm, which is the height of the fibrils. The smaller η, the more important the nano-structures are to the mean roughness. For η values of 1e1 and 1e0, only the nano-structures remain. In these cases, the mean roughness allows for a clear distinction between UNS and EPY. The corresponding mean roughnesses R_a for UNS and EPY are 0.39 ± 0.07 and 0.13 ± 0.03 nm, respectively. The sizing appears to cover the nano-structures. For η = 1e0, R_a will in the following be called nano-roughness, $R_{a,n}$.

Nanoscale topography analysis

Generally, for small values of η, higher values of $R_{a,n}$ are due to more rapid changes in the height signal. One reason for these rapid changes are nano-structures. A second reason is the border between two fibrils, since the transition between them is often similar to a kink in the height signal rather than to a smooth transition. To visualize the origin of the roughness, at every point of the corrected image, the absolute difference between the height of the point and the mean height of the image is computed. This value will be called total background corrected height (TBH). For η = 1e0, the sum over all TBH divided by the total number of points would result in the nano–roughness, $R_{a,n}$

$$\mathrm{TBH} = \left| y_{i,\mathrm{corr}} - \langle y_{\mathrm{corr}} \rangle \right| \tag{5}$$

$$R_{a,n} = \frac{\sum_{i=1}^{N} \mathrm{TBH}}{A} \tag{6}$$

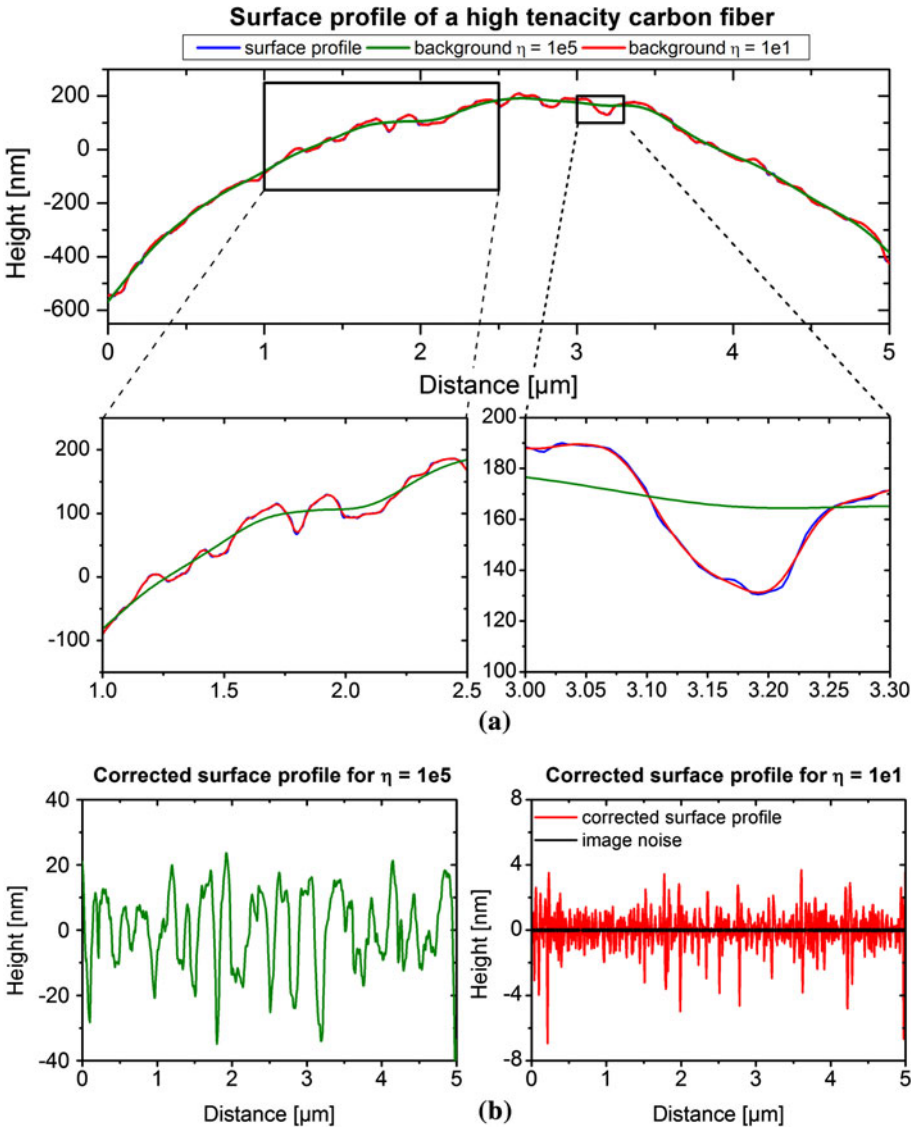

Fig. 3 **a** Surface profile (*blue line*, see Fig. 2) and corresponding backgrounds for η values of 1e5 (*green line*) and 1e1 (*red line*), **b** corrected surface profiles for η values of 1e5 and 1e1 (different height scales). In the case of η = 1e1, the measured image noise is shown for comparison (Color figure online)

Table 2 Summary of the mean roughnesses R_a of background corrected surface images of UNS and EPY for different values of η

η	R_a^{UNS} (nm)	R_a^{EPY} (nm)
1e6	16.76 ± 4.63	16.26 ± 4.17
1e5	10.65 ± 2.64	9.63 ± 3.26
1e4	6.42 ± 1.31	4.71 ± 1.57
1e3	3.51 ± 0.67	1.96 ± 0.61
1e2	1.75 ± 0.39	0.77 ± 0.23
1e1	0.82 ± 0.20	0.30 ± 0.07
1e0	0.39 ± 0.07	0.13 ± 0.03

The mean values and standard deviations are calculated from ten measurements each. The considered scale of the structures for the different values of η can be seen in Table 1

with $y_{i,\mathrm{corr}}$ being the corrected height of one data point, $\langle y_{\mathrm{corr}} \rangle$ the mean value of the corrected height data, and A the total number of points within the image.

Figure 4a–f shows images of the EPY, UNS, and EPYdeMEK fibers. The grayscale background (scale −50 to 50 nm) was formed from a background corrected AFM image (size 5 × 5 μm) with a η value of 1.8e6. Mainly fibrils with a width of ∼100 nm are observable. The total background corrected height values for each point of the image are displayed in color, background corrected with an η value of 1e0 and colored according to the displayed colorbar (in nm). For better visibility, TBH values below 0.3 nm are transparent. Figure 4a, c, and e shows two-dimensional projections (size 5 × 5 μm), and Fig. 4b, d, and f shows the corresponding three-dimensional zoom-ins (size ∼0.3 × 0.3 μm). The position of the zoom-ins is marked by a red rectangle in the respective figures. The nano-roughnesses of the images are 0.35 nm for UNS, 0.10 nm for EPY, and 0.44 nm for EPYdeMEK.

Comparing UNS and EPY (Fig. 4a, c), the fibrils can clearly be seen in both cases. A more detailed view of the

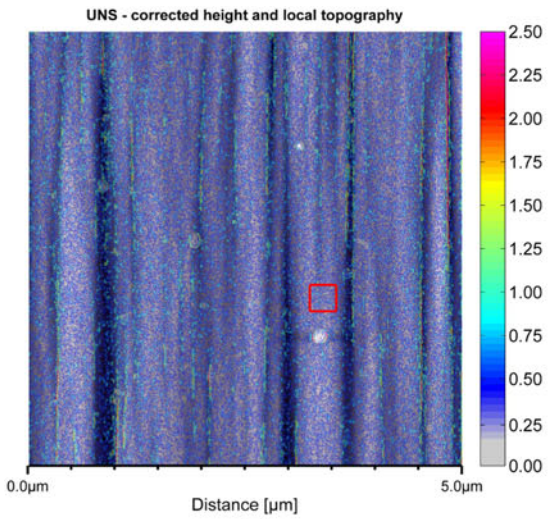
UNS - corrected height and local topography
0.0μm
5.0μm
Distance [μm]
2.50
2.25
2.00
1.75
1.50
1.25
1.00
0.75
0.50
0.25
0.00

(a)

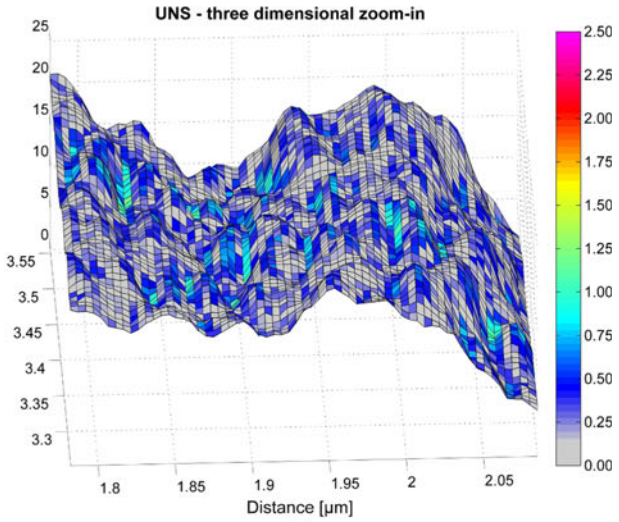
UNS - three dimensional zoom-in
Distance [μm]

(b)

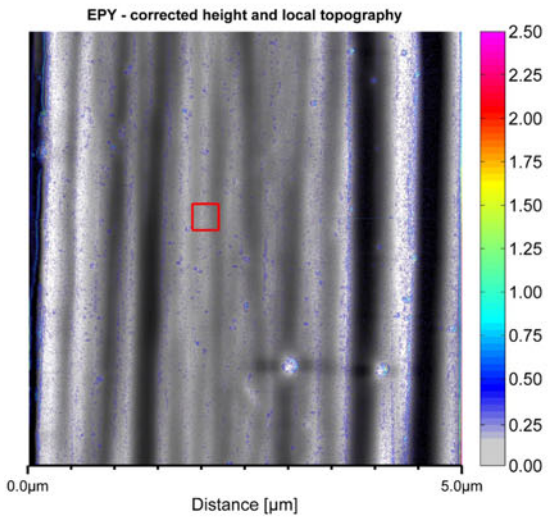
EPY - corrected height and local topography
0.0μm
5.0μm
Distance [μm]

(c)

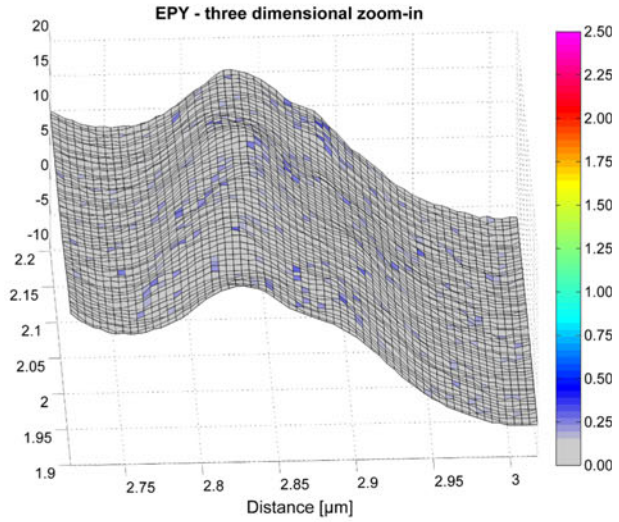
EPY - three dimensional zoom-in
Distance [μm]

(d)

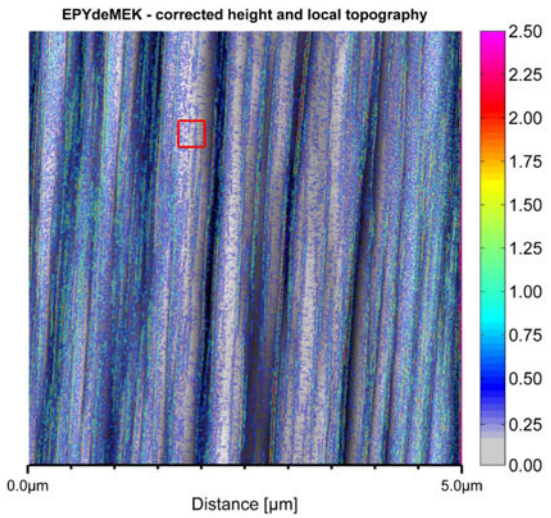
EPYdeMEK - corrected height and local topography
0.0μm
5.0μm
Distance [μm]

(e)

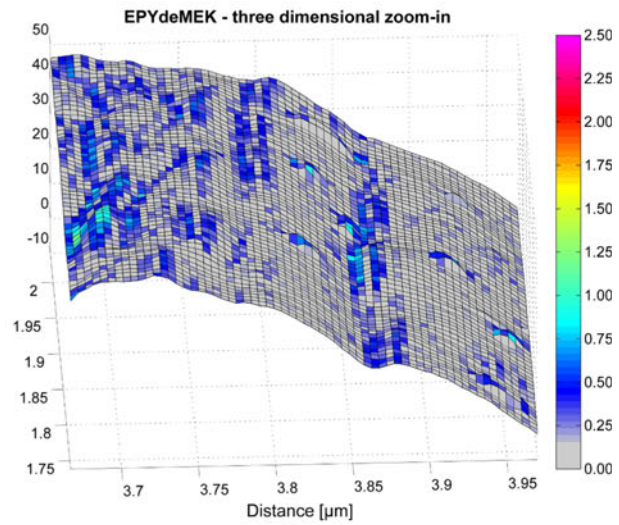
EPYdeMEK - three dimensional zoom-in
Distance [μm]

(f)

◀ **Fig. 4** **a**, **c**, and **e** show in grayscale a two-dimensional projection of the fiber surface, background corrected with η = 1.8e6 (background, scale −50 to 50 nm) and in *color* the total background corrected height (TBH) for each point after background correction with η = 1e0 (*colored* according to *colorbar*; units: nm, foreground) for UNS (unsized), EPY (sized), and EPYdeMEK (desized), respectively, **b**, **d**, and **f** respective three-dimensional zoom-ins of the *red rectangles*. *Units* distance (x and y axes) in μm, and height (z axes) in nm (Color figure online)

surface is obtained from the respective three-dimensional zoom-ins. The surface of UNS is very rough with plenty of nano-structures of around 20 nm in size (Fig. 4b). The colored total background corrected height values represent the hills and valleys of these nano-structures. In Fig. 4a, these nano-structures, represented by the mostly blue colored TBH values, are evenly distributed over the fibrils of the unsized fiber. The sized fiber does not show any of these nano-structures; the three-dimensional zoom-in only shows a flat and smooth surface and there are almost no colored parts in Fig. 4c. The nano-structures were also expected to appear in the case of the desized fiber. Although, this is true for the fibrils at the edges of image 4e, only a few nano-structures are present on the fibrils in the center of the image (compare Fig. 4e, f).

Concerning measurement artifacts image noise only affects slightly the measured nano-roughness as was checked by a test measurement on an atomically flat surface (compare Fig. 3b). For all reasonable gain settings, the surface roughness of the sized fiber remains significantly smaller than that of the unsized fiber.

The presented total background corrected height analysis allows the evaluation of the distribution, size, and height of nano-structures on an arbitrary surface. This feature, for example, not only allows us to distinguish between sized and unsized fibers, but also to visualize the distribution of sizing on a fiber and even on a fibril.

Spatial distribution of nano-structures

In the current roughness analysis, R_a and $R_{a,n}$ are "global" values for the whole image, whereas the visualization of the TBH is local. The starting of a new fibril presents as a rapid change in the height signal, often more rapid than in the case of nano-structures, causing high-total background corrected height values. This leads to overestimation of the nano-roughness, because a high $R_{a,n}$ value is not only caused by nano-structures. To filter out these artificial features, a further analysis which considers the spatial distribution of the nano-structures is done. For this purpose, the local regional maxima and minima of the background corrected height data are counted (both are needed because we have a symmetric background), and classified according to their total background corrected height values, TBH, in different classes, hereafter called peaks and peak-classes. Due to the symmetric background correction, the total background corrected height of these peaks is half the height of the previously shown nano-structures. For every peak- class, the aggregation index R, defined by Clark and Evans [15], is computed to analyze the lateral distribution of peaks within a peak- class:

$$R = \frac{\bar{r}_{\text{observed}}}{E(r)}; \quad E(r) = \frac{1}{2\sqrt{\frac{N}{A}}}; \quad R \in [0; 2.14] \tag{7}$$

In this formula $\bar{r}_{\text{observed}}$ describes the mean distance peak–nearest neighbor peak, $E(r)$ the mean distance for a Poisson distribution, N the total number of peaks (within the peak-class), and A the area (in our case 1024 × 1024 pixels). Values of R below 1 represent an aggregation of the peaks within a peak- class, values around 1 a random distribution, and values above 1 regular distribution. The lower the value of R, the stronger the clustering of the peaks. Table 3 summarizes the mean values of N, $\bar{r}_{\text{observed}}$, and R for ten measurements of UNS, EPY, and EPYdeMEK.

Table 3 Peak analysis for ten measurements for UNS, EPY, and EPYdeMEK. N is the total number of peaks within the peak-class, $\bar{r}_{\text{observed}}$ the mean distance peak–nearest neighbor peak (in nm), R the aggregation Index defined by Eq. (7), and $R_{a,n}$ the roughness R_a of the respective samples calculated with an η-value of 1e0

Peak-classes	UNS			EPY			EPYdeMEK		
	N	$\bar{r}_{\text{observed}}$ (nm)	R	N	$\bar{r}_{\text{observed}}$ (nm)	R	N	$\bar{r}_{\text{observed}}$ (nm)	R
TBH > 5nm	309	56	0.13	158	14	0.06	679	13	0.12
2.5nm < TBH < 5nm	1088	20	0.25	329	15	0.10	2283	18	0.32
1nm < TBH < 2.5nm	11994	16	0.69	1482	17	0.24	20062	14	0.78
0.75nm < TBH < 1nm	15293	18	0.87	1256	29	0.36	13572	18	0.85
0.5nm < TBH < 0.75nm	30350	15	1.01	4460	21	0.52	22308	16	0.94
0.25nm < TBH < 0.5nm	34294	13	0.98	34263	13	0.98	30795	14	0.95
0.1nm < TBH < 0.25nm	13679	19	0.85	101008	9	1.14	18207	17	0.83
Nano-roughness $R_{a,n}$ (nm)	0.39 ± 0.07			0.13 ± 0.03			0.46 ± 0.10		

All given values are mean values. In the case of the nano-roughness $R_{a,n}$ the standard deviation is specified in addition to the mean value

The nano-roughnesses of UNS and EYPdeMEK are identical within the error , whereas the nano-roughness of EPY is only one third of it. The number of peaks, *N*, for EPY raises the smaller TBH, whereas for UNS and EPYdeMEK, no clear trend for values of TBH below 2.5 nm can be found.

The number of peaks within a peak-class has to be correlated with the aggregation index *R*. Small values of *R* (below 0.6) indicate that these peaks are heavily clustered and in our case, mainly exist at the start of a fibril and so do not belong to the "real" nano-roughness of the sample, but rather to the background correction itself. Values of *R* above 0.8 indicate a random distribution. Comparing this index for EPY, UNS, and EPYdeMEK, EPY only has random peaks for TBH values below 0.5 nm, whereas UNS and EPYdeMEK have random peaks up to a total background corrected height of 2.5 nm. The number of peaks with the respective Aggregation Index proves that the unsized and desized fibers have real nano-structures up to a height of 5 nm (the value of TBH must be doubled because of the use of a symmetric background correction).

Thus, the presented analysis of the spatial distribution of the nano-structures allows us to distinguish between real nano-structures and artificial structures. Combining this analysis with the calculated nano-roughness, one is able to filter out the artificial component and define a real nano-roughness for the surface of the sample.

Conclusion

This study presents a method which allows the analysis of structures of widely varying scales on an arbitrary surface. The thereby presented tunable background is used to subtract all the structures down to a freely chosen size while finer structures remain unchanged for further analysis. It is thus possible to perform a real multiscale analysis. The method is herein applied to analyze roughness (microscale) and nano-roughness (nanoscale) of unsized, sized, and desized high-tenacity carbon fibers. Unsized fibers have plenty of evenly distributed nano-structures whereas sized fibers do not show any. Evaluating the total background corrected height allows the visualization of the distribution, width, and height of these nano-structures for the first time. Areas, where nano-structures are absent, are a signature for the presence of the sizing and therefore this method allows the evaluation of the distribution of sizing on a carbon fiber surface. This effect is demonstrated on desized fibers. The lateral resolution for the total background corrected height analysis is limited by the lateral resolution of the microscope.

With the presented method, it is now possible to correlate the surface structures to parameters used during carbon fiber production processes and/or to evaluate the contribution of mechanical interlocking to the interfacial strength.

Acknowledgements Special thanks are addressed to Christina Kunzmann for her ideas in the initial phase of this study and to Markus Sause for many fruitful discussions.

References

1. Bischof C, Possart W (1983) Adhäsion: theoretische und experimentelle Grundlagen. Akademie-Verlag
2. Latella B, Perera D, Escott T, Cassidy D (2006) J Mater Sci 41(4):1261. doi:10.1007/s10853-005-4234-3
3. Fernandez B, Arbelaiz A, Valea A, Mujika F, Mondragon I (2004) Polym Compos 25(3):319
4. Jones FR (2010) J Adhesion Sci Technol 24(1):171
5. Dilsiz N, Wightman JP (1999) Carbon 37(7):1105
6. Yang Y, Lu C, Su X, Wang X (2007) J Mater Sci 42(15):6347. doi:10.1007/s10853-006-1198-x
7. Lin S, Yip F (1989) 19th Biennial conference on carbon, vol session 2A, pp 244245
8. Shahrul SN, Hartini MN, Hilmi EA, Nizam A, Rusop M, Subban RY, Kamarulzaman N, Wui WT (2010) AIP Conference Proceedings, vol 1217, pp 472477
9. Drzal LT, Sugiura N, Hook D (1996) Compos Interfaces 4(5):337
10. Liu CH, Nairn JA (1999) Int J Adhesion Adhesives 19(1):59
11. Hampe A, Marotzke C (1997) J Reinf Plast Compos 16(4):341
12. Hampe A, Kalinka G, Meretz S, Schulz E (1995) Composites 26(1):40
13. Eilers PH (2003) Anal Chem 75(14):3631
14. Eilers PH (2004) Anal Chem 76(2):404
15. Clark PJ, Evans FC (1954) Ecology 35(4):445